



HAL
open science

Visible Luminescence from Octadecylsilane Monolayers on Silica Surfaces : Time-Resolved Photoluminescence Characterization

T. Uchino, N. Sagawa

► **To cite this version:**

T. Uchino, N. Sagawa. Visible Luminescence from Octadecylsilane Monolayers on Silica Surfaces : Time-Resolved Photoluminescence Characterization. ENS 2006, Dec 2006, Paris, France. pp.5-8. hal-00166755

HAL Id: hal-00166755

<https://hal.science/hal-00166755>

Submitted on 9 Aug 2007

HAL is a multi-disciplinary open access archive for the deposit and dissemination of scientific research documents, whether they are published or not. The documents may come from teaching and research institutions in France or abroad, or from public or private research centers.

L'archive ouverte pluridisciplinaire **HAL**, est destinée au dépôt et à la diffusion de documents scientifiques de niveau recherche, publiés ou non, émanant des établissements d'enseignement et de recherche français ou étrangers, des laboratoires publics ou privés.

VISIBLE LUMINESCENCE FROM OCTADECYLSILANE MONOLAYERS ON SILICA SURFACES: TIME-RESOLVED PHOTOLUMINESCENCE CHARACTERIZATION

Takashi Uchino and Natsuko Sagawa

Department of Chemistry, Faculty of Science, Kobe University, Kobe 657-8501, Japan, and SORST, Japan Science and Technology Agency, Kawaguchi, Saitama 332-0012, Japan

ABSTRACT

We have found that the adsorption of octadecyltrichlorosilane (OTS) monolayers on nanometer-sized silica particles yields a stable blue photoluminescence (PL) with a time scale of nanoseconds. The observed PL intensity increases after curing at temperatures from ~ 100 to ~ 300 °C, suggesting that condensations between adjacent OTS molecules on the silica surface are related to the PL. The PL decay curve of the cured samples remains unchanged from 77 to 450 K, whereas the time-integrated PL intensity shows a monotonous decrease with increasing temperature. From these experimental results, a model of radiative and nonradiative process associated with the PL is presented.

1. INTRODUCTION

Blue photoluminescence (PL), which is characterized by single-exponential [1] or multi-exponential decay [2] on the order of nanoseconds, has been reported from a variety of porous silicon such as aged, chemically oxidized and thermally oxidized samples [3]. Although there still exists an argument that the blue PL is explained by a quantum confined mechanism [4], the weight of evidence is in favor of a defect-related model [3,5]. Some researchers suggest that C-related defects are responsible for the blue PL characteristics [2,6]. Others alternatively claim that the presence of OH groups adsorbed on the surface of porous silicon are associated with this type of output [7]. Although the physical origin of the blue PL band in porous Si has not been unambiguously clarified yet, it is quite likely that C- and/or OH-related surface defects play crucial role, either directly or indirectly, in exhibiting the blue PL band.

It is hence reasonable to assume that the blue PL emission can be obtained when C- and/or OH-based species are intentionally introduced into the oxidized Si species or SiO₂-based materials. Under this concept, various organic/inorganic hybrid SiO₂ xerogels showing the blue-green PL emission were previously synthesized by sol-gel method [8-11]. The obtained PL characteristics are quite analogous to those of oxidized porous silicon, suggesting that both the PL emissions result from a similar origin. These organic/inorganic sol-gel materials

are certainly interesting in terms especially of low-cost manufacturing; however, the expected instability owing to their porous nature may become a major problem for general device use.

To circumvent the problem of the sol-gel derived xerogels, we here use a silanization reaction of silica surface with octadecyltrichlorosilane (CH₃(CH₂)₁₇-SiCl₃, OTS). OTS has been extensively used as a silanizing reagent for forming self-assembled monolayers (SAMs) on silica-based substrate or metals with oxide coatings, showing high stability and resistance to mechanical, thermal, and environmental attacks [12,13]. The driving force for the spontaneous formation of stable OTS SAMs comes from the adsorption of the headgroup of OTS molecules with the surface and hydrophobic intermolecular interactions of the alkyl chains. It is also interesting to note that the spontaneous adsorption of OTS molecules on the silica substrates is irreversible, leading to the hydrolyzed OTS molecules that are strongly attached via hydrogen bonds to the OH groups on the silica surface and neighboring OTS molecules [14]. Thus, the OTS-modified silica is highly stable under prolonged storage and is also expected to show a blue PL emission as in the case of organic/inorganic silica xerogels and oxidized porous silicon.

In this work, we report PL characteristics of OTS SAMs on nanometer-sized amorphous silica particles using the steady-state and time-resolved PL spectroscopy [15]. Emphasis is given to the PL characteristics and its correlation with the surface condensation reaction. We also carry out temperature dependent PL measurements to give a detailed picture of the observed PL phenomena.

2. EXPERIMENTAL PROCEDURES

Amorphous silica particles employed were a nonporous fumed silica (Aerosil 380) obtained from Nippon Aerosil Co., LTD. It had a nominal surface area of 380 ± 30 m²/g and a average primary particle size of 7 nm (product specification). We have recently shown that the structural and optical characteristics of fumed silica are interesting in its own right [16], but we here use it as a silica substrate with a large specific surface area. OTS SAMs were prepared according to the literature method [17]. Adsorption was initiated by the addition of 6 g of OTS to

100 mL of anhydrous pentane containing 2 g of fumed silica. The reaction mixture was stirred for 4 h at room temperature and transferred to centrifuge tubes. The stoppered tubes were centrifuged and the solution was decanted. The samples were washed with fresh anhydrous pentane to remove unreacted OTS. The resulting samples were then dried at room temperature. All the above procedures were carried out in a glovebox that was purged with argon. For the subsequent curing step, the powdered samples were compacted at 530 MPa into a disk-shaped pellet of 19.3 mm in diameter and averaging 0.9 mm in thickness. The curing was performed in N₂ atmosphere in the temperature range from 150 to 600 °C for 2 h.

Steady state PL spectra were measured at room temperature with a spectrofluorometer (Photon Technology International, QM-2000-3) using a pulsed xenon source for excitation. Time-resolved PL measurements were also performed using a synchroscan streak camera (Hamamatsu, C4334) and the second harmonic (350 nm) pulse of a mode-lock Ti:sapphire laser (Spectra-Physics, Tsunami) with a repetition rate of 1 MHz, an average power of 0.3 mW and typical pulse lengths of < 180 fs. The sample temperature was varied between 77 and 450 K in a closed-cycle N₂ cryostat.

3. RESULTS AND DISCUSSION

Figure 1 shows the steady state PL spectra of as-prepared and cured samples under 350-nm excitation. The measurements were carried out at room temperature. Although the as-prepared sample only shows a weak PL response below ~500 nm, the blue PL band peaking at ~420 nm is clearly evident for the cured samples. The intensity of the blue PL band tends to increase with increasing temperature up to 300 °C, whereas the PL is almost quenched after curing treatment at temperature of 600 °C. The PL emission from the cured samples is quite stable and shows no aging effects after exposure to the ambient environment for more than 6 months. These spectral features along with the temperature dependence are rather different from those reported previously for fumed silica itself [18], indicating that the observed PL does not result from possible PL centers derived from the original fumed silica surface.

Figure 2 illustrates the time decay of the PL of the sample cured at 200 °C. The PL decay is obtained at the peak of the emission. We see from Fig. 2(a) that the decay is nonexponential and can be tentatively fitted by a double exponential function, yielding time constants of ~4 and ~18 ns at 77 K. The decay curve varies little with the detection wavelength throughout the blue band. It should also be worth mentioning that there is no

significant variation in decay time within experimental

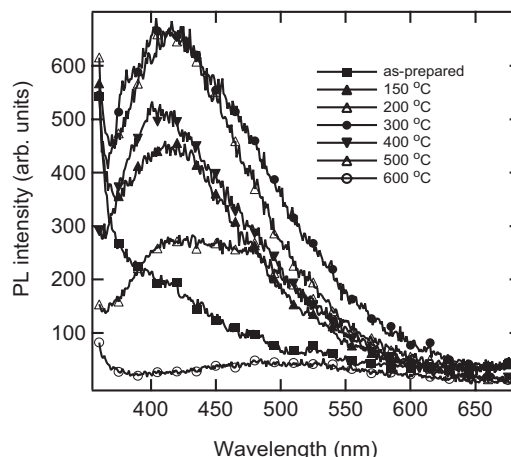


Figure 1. Steady-state PL spectra of OTS SAMs on fumed silica before and after curing at the respective temperatures indicated. The excitation wavelength is 350 nm. The measurements were performed at room temperature.

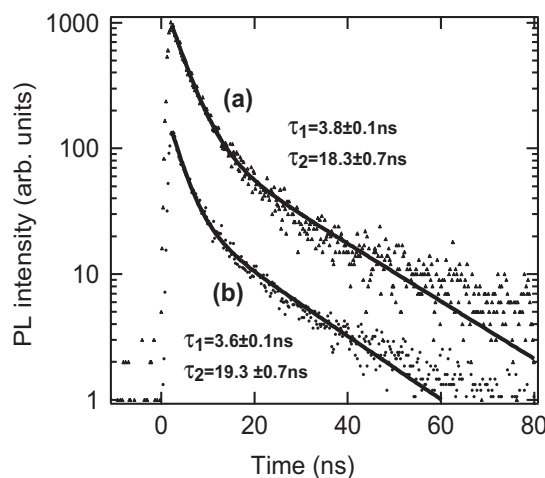


Figure 2. PL decay curves for OTS SAMs on fumed silica after curing at 200 °C measured at (a) 77 and (b) 450 K. The excitation source is the second harmonic (350 nm) of the pulsed Ti:sapphire laser. The time resolution of the system is < 200 ps. The experimental data are fitted with a double exponential function with time constants τ_1 and τ_2 and shown as solid line.

error in the temperature range employed (77-450 K) [see, for example, Fig. 2(b)]. On the other hand, the time-integrated PL intensity shows a monotonic decrease with increasing temperature as shown in Fig. 3.

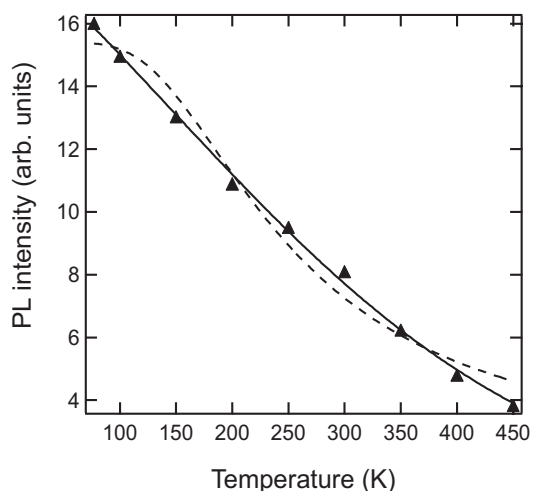


Figure 3. Temperature dependence of the integrated PL intensity for OTS SAMs on fumed silica cured at 200 °C. The dashed and solid lines are least square fits with Eqs. (1) and (2), respectively.

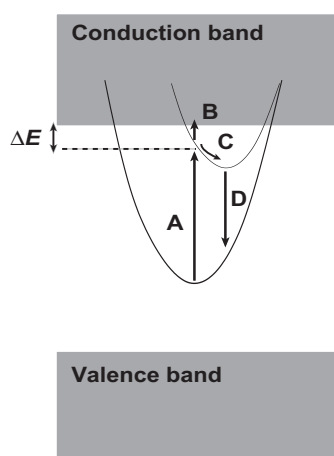


Figure 4. Schematic configuration coordinate diagram for the defect-related ground and excited states accounting for the temperature-independent PL lifetime and the temperature-dependent PL intensity (adapted after Ref. 19).

On the basis of the above experimental results, we discuss the PL mechanism of the present samples. According to previous studies on OTS SAMs, curing at temperatures from 120 to 200 °C has an effect to promote the condensation between adjacent adsorbed OTS molecules rather than the condensation between the surface silanols and adsorbed alkylsilanols [14]. The

curing treatment hence induces the cross-linking reaction via intermolecular Si-O-Si linkage to form well-ordered SAMs. It has also been demonstrated that such a cross-linked Si-O-Si bond between adjacent adsorbed OTS molecules is highly strained because of the geometry constraints imposed by the well-ordered SAMs [14]. These highly strained Si-O-Si bonds created during curing can be viewed as defective oxide structures. We hence suggest that the present PL output results from these surface defective oxide bonds. However, curing at temperatures more than ~500 °C will partly decompose the alkyl groups of OTS, leading to the relaxation of the strained Si-O-Si and the concomitant quenching of the blue PL emission as shown in Fig. 2. These results allow us to conclude that as far as the present OTS SAMs are concerned, the carbon-related structures are not necessarily needed to exhibit the blue PL but may have an effect to stabilize the surface defective PL centers.

We shall next concentrate our interest on the PL decay dynamics shown in Fig. 2. As mentioned earlier, the present samples do not show any significant change in decay time with temperature. Such a temperature-independent decay is observed in the blue PL from porous silicon as well [1]. We should note, however, that the integrated PL intensity is highly dependent on temperature as shown in Fig. 3, suggesting that a temperature dependent nonradiative pathway is certainly involved in the entire excitation and recombination processes.

It is interesting to note that such PL characteristics, namely, the temperature-independent lifetime and the temperature-dependent intensity, have also been reported for a defect-related emission in Si-doped GaAs [19]. The observed phenomena have been interpreted in terms of the localized state emission [19]; the schematic configuration coordinate diagram proposed to account for the observations is shown in Fig. 4. The electrons in the defect ground state are excited to the defect excited state by absorbing incident photons (process A in Fig. 4). Some of the excited electrons will be thermally promoted to the continuum conduction band (process B in Fig. 4) and will eventually lose their excess energy as nonradiative recombination. The rest of the excited electrons will be able to relax to the bottom of the defect excited state (process C in Fig. 4). Provided that the bottom of the defect excited state is located well below the conduction states, the electrons in the bottom of the defect excited state will not be thermally activated into the conduction states but will solely lead to the radiative emission (process D in Fig. 4). Consequently, the radiative process D does not compete with any of the existing nonradiative processes. The overall scheme shown in Fig. 4 can thus account for the decreasing PL intensity with increasing temperature without any change

in the decay time and is, therefore, expected to be applied to the present defect-related PL emission as well. As already mentioned, the defect states relevant to the present emission process will be highly strained Si-O-Si bonds created during condensation of adjacent OTS molecules.

According to the above energy state model, the temperature dependence of the PL intensity can be simply represented as follows [20]:

$$I_{\text{PL}} \propto \tau_{\text{R}}^{-1} / (\tau_{\text{R}}^{-1} + \tau_{\text{NR}}^{-1}) = [1 + A \exp(-\Delta E / kT)]^{-1} \quad (1)$$

where τ_{NR} and τ_{R} are the lifetime of the non-radiative (process B) and radiative (process D) recombinations, respectively, A is a temperature-independent prefactor, and ΔE is the activation energy of the non-radiative process. From the least-square fit of Eq. (1) to the measured data, the value of ΔE is estimated to be 0.062 ± 0.005 meV, which corresponds to the energy separation between the upper level of the defect excited state and the bottom of the conduction band according to the scheme shown in Fig. 4. We have to admit, however, that the fitting of the data with Eq. (1) (see the dashed line in Fig. 3) is not perfect over the entire temperature range examined, suggesting a distribution of ΔE . When there exists a distribution of activation energies for nonradiative recombination, another equation has been proposed to represent the temperature dependence of the PL intensity, namely [21],

$$I(t) \propto [1 + A \exp(T/T_0)]^{-1}, \quad (2)$$

where T_0 is a characteristic temperature that is inversely correlated to the slope of the density-of-states distribution, $g(\varepsilon)$, below the conduction band edge. We see from Fig. 4 that Eq. (2) can fit the data much better than Eq. (1); the fitted value of T_0 is 139 K. A rather high value of T_0 implies a gentle slope of $g(\varepsilon)$ and hence a wide distribution of ΔE as expected.

4. CONCLUSIONS

In conclusion, we present the stable blue PL emission from OTS SAMs. The PL intensity has been found to increase with increasing curing temperature up to ~ 300 °C, implying that the cross-linking reaction of OTS molecules are related to the PL. We propose that the highly strained defective siloxane bonds that are formed during cross-linking are responsible for the blue PL emission. Furthermore, our PL data are interpreted in terms of the defect-level recombination model, giving a semi-quantitative picture of the energy levels involved in the emission. We should note, however, that the observed

PL decay curve cannot be represented by a pure exponential function, suggesting the actual PL processes are not simple as shown in Fig. 4 but may result from a feeding of the radiative transition from some reservoir or trap states. More works are now in progress to get the complete energy level structure associated with the PL.

This work was supported by grants from the Ministry of Education, Culture, Sports, Science and Technology, Japan (No. 14350352) and Toray Science Foundation.

References

- [1] C. I. Harris, M. Syväjärvi, J. P. Bergman, O. Kordina, A. Henry, B. Monemar, and E. Janzén, *Appl. Phys. Lett.* **65**, 2451 (1994).
- [2] L. T. Canham, A. Loni, P. D. J. Calcott, A. J. Simons, C. Reeves, M. R. Houlton, J. P. Newey, K. J. Nash, and T. I. Cox, *Thin Solid Films* **276**, 112 (1996).
- [3] A. G. Cullis, L. T. Canham, and P. D. J. Calcott, *J. Appl. Phys.* **82**, 909 (1997).
- [4] H. Koyama and N. Koshida, *Solid State Commun.* **103**, 37 (1997).
- [5] L. Tsybeskov, Ju. V. Vandyshev, and P. M. Fauchet, *Phys. Rev. B* **49**, 7821 (1994).
- [6] A. J. Kontkiewicz, A. M. Kontkiewicz, J. Siejka, S. Sen. G. Nowak, A. M. Hoff, P. Sakthivel, K. Ahmed, P. Mukherjee, S. Witanachchi, and J. Lagowski, *Appl. Phys. Lett.* **65**, 1346 (1994).
- [7] H. Tamura, M. Rückschloss, T. Wirschem, and S. Vepřek, *Appl. Phys. Lett.* **65**, 1537 (1994).
- [8] W. H. Green, K. P. Le, J. Grey, T. T. Au, and M. J. Sailor, *Science* **276**, 1826 (1997).
- [9] J. Lin, and K. Baerner, *Mat. Lett.* **46**, 86 (2000).
- [10] H. He, Y. Wang, and H. Tang, *J. Phys.:Condens. Matter* **14**, 11867 (2002).
- [11] L. D. Carlos, R. A. Sá Ferreira, R. N. Pereira, M. Assunção, and V. de Zea Bermudez, *J. Phys. Chem. B* **108**, 14924 (2004).
- [12] A. Ulman, *Adv. Mater.* **2**, 573 (1990).
- [13] A. N. Parkikh, J. D. Beers, A. P. Shreve, and B. I. Swanson, *Langmuir* **15**, 5369 (1999).
- [14] C. P. Tripp and M. L. Hair, *Langmuir* **11**, 1215 (1995).
- [15] N. Sagawa and T. Uchino, *Appl. Phys. Lett.* **87**, 251923 (2005).
- [16] T. Uchino, A. Aboshi, S. Kohara, Y. Ohishi, M. Sakashita, and K. Aoki, *Phys. Rev. B* **69**, 155409 (2004); T. Uchino and T. Yamada, *Appl. Phys. Lett.* **85**, 1164 (2004); T. Yamada and T. Uchino, *Appl. Phys. Lett.* **87**, 081904 (2005); T. Uchino, N. Kurumoto, and N. Sagawa, *Phys. Rev. B* **73**, 233233 (2006).
- [17] R. Wang and S. L. Wunder, *Langmuir* **16**, 5008 (2000).
- [18] A. S. Zyubin, Yu. D. Glinka, A. M. Mebel, S. H. Lin, L. P. Hwang, and Y. T. Chen, *J. Chem. Phys.* **116**, 281 (2002).
- [19] T. Sauncy, C. P. Palsule, M. Holtz, and S. Gangopadhyay, *Phys. Rev. B* **53**, 1900 (1996).
- [20] M. S. Minsky, S. Watanabe, and N. Yamada, *J. Appl. Phys.* **91**, 5176 (2002).
- [21] R. W. Collins and W. Paul, *Phys. Rev. B* **25**, 5257 (1982).